Testing the Potential Model in the Υ System[1]

SUSAN COOPER[2]

In this talk I will discuss tests of the non-relativistic potential model for bound $b\bar{b}$ states, using results from the Crystal Ball and ARGUS detectors at DORIS II (DESY) and the CUSB and CLEO detectors at CESR (Cornell). There are many many people who have developed potential models. While I will try to be complete in reviewing the experimental data, I will limit my discussion of potentials to a few contrasting examples.

The talk is divided into two main parts. In the first I discuss the $^3S_1$ $b\bar{b}$ states Υ, Υ′, ..., whose measured masses, leptonic widths, and leptonic branching ratios are used to check the static potential V(r) and the strong coupling constant α_s. In the second part, results on the ^3P_J $b\bar{b}$ states χ_b, χ_b' are used to check the spin dependence of the potential. There are several other classes of states ($c\bar{c}$, $s\bar{s}$, $c\bar{q}$, $b\bar{q}$, and the as-yet-not seen η_b and $^1P_1$ of the $b\bar{b}$ family) which are also important in testing the potential model, but which I cannot cover in this talk.

1. The Υ Family

The Υ was discovered in $\mu^+\mu^-$ final states of hadron reactions (Ref. 1). More data taken by the same experiment gave indications for two more resonances, the Υ′ and the Υ″ (Ref. 2). Much better resolution and signal-to-background ratio is obtained in $e^+e^- \to hadrons$, and it is from this process that we now have most of our information about the Υ family. The Υ and the Υ′ were confirmed at DORIS (Ref. 3). At CESR, the Υ″ was confirmed (Ref. 4), and further members of the Υ family have been found (Ref. 5, 6, 7).

[1]Invited Talk presented at the SLAC Topical Conference, August 1984.
Work supported by the Department of Energy.
[2]Stanford Linear Accelerator Center, Stanford University, Stanford, California
mailing address: DESY, Notkestraße 85, D-2000 Hamburg 52, W. Germany

Typical resonance curves from $e^+e^- \rightarrow$ *hadrons* are shown in Figure 1. The first three resonances Υ, Υ', and Υ'' are very narrow: the width you see in the figure is due to the energy spread of the beam.

The mass of each resonance is determined by correlating the peak of the $e^+e^- \rightarrow$ *hadrons* cross section with the beam energy. When the beam energy is determined from the ring magnet currents, there is a systematic uncertainty of 0.1-0.3%. When beam polarization is present (dependent on energy and details of the ring) the beam energy can be determined very precisely by measuring the frequency of the additional magnetic field needed to destroy the polarization. This technique was developed at Novosibirsk (Ref. 8) and has been used there and at DORIS and CESR to measure the Υ, Υ' and Υ'' masses. The results are given in Table 1.

Table 1. Measurements of the Υ Masses in MeV/c^2

$\Upsilon(1S)$	$9460.6 \pm 0.4 \pm < 0.2$	depol.	VEPP-4	Ref. 9
	$9460.0 \pm 0.1 \pm 0.1$	depol.	CESR	Ref.10
	$\overline{9460.1 \pm 0.2}$		average	
$\Upsilon'(2S)$	$10023.1 \pm 0.4 \pm 0.1$	depol.	DORIS	Ref. 11
	$10023.8 \pm 0.5 \pm < 0.2$	depol.	VEPP-4	Ref. 9
	$\overline{10023.4 \pm 0.4}$		average	
$\Upsilon''(3S)$	$10355.5 \pm 0.5 \pm < 0.2$	depol.	VEPP-4	Ref. 9
$\Upsilon'''(4S)$	$10578 \pm 1 \pm 4$	(prel.)	CLEO	Ref. 6
	$10577 \pm 1 \pm ?^*$	(prel.)	CUSB	Ref. 7
	$\overline{10577 \pm 4}$		average	
$\Upsilon''''(5S?)$	$10868 \pm 6 \pm 5$	(prel.)	CLEO	Ref. 6
	$10845 \pm 20 \pm ?^*$	(prel.)	CUSB	Ref. 7
	$\overline{10863 \pm 10}$		average	

* systematic error not yet known

The Υ''', which is above the threshold for decay to $B\bar{B}$ mesons, is seen as a considerably weaker and wider resonance (Fig. 1a). With the expanded vertical axis of Figure 1b, one sees a still smaller peak near 10.86 GeV, which may be

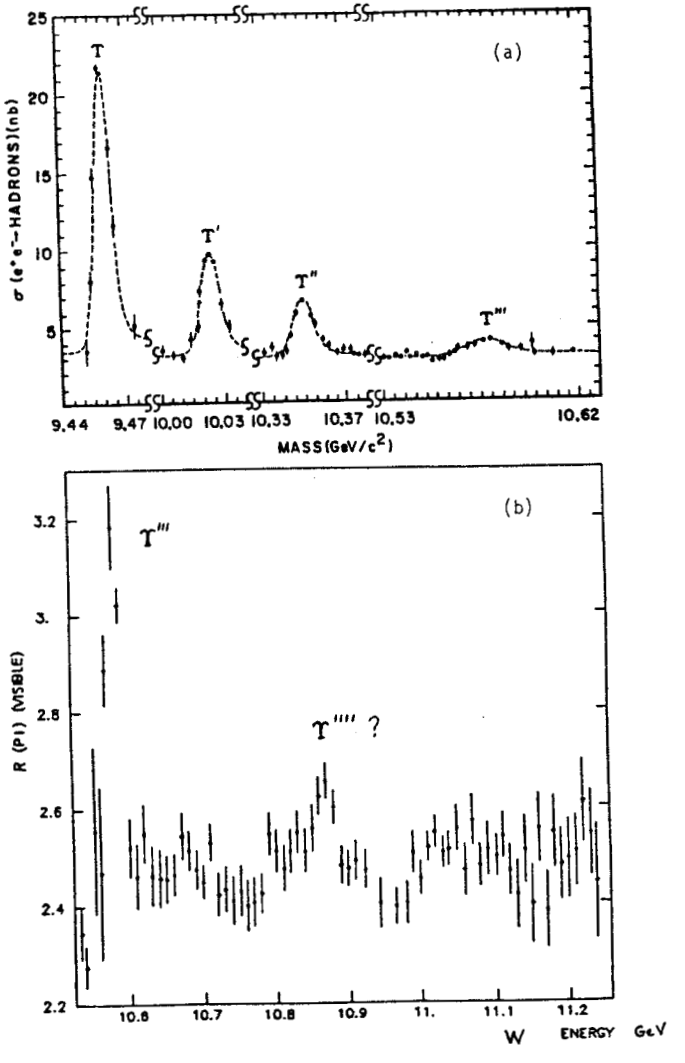

Figure 1. Resonances of Υ in $e^+e^- \rightarrow$ *hadrons* (CUSB data).

the Υ'''', and perhaps yet more structure due to $B_s\bar{B}_s$, etc. thresholds. In this complicated region, the separation of peak from background can be ambiguous, leading to model-dependent uncertainties, especially for the strengths of the resonances.

The Potential Model

Such a large collection of related resonances requires an explanation, i.e. a calculation which gives the measured resonance parameters. We believe that these resonances are bound states of $b\bar{b}$, which should be easier to describe than other mesons because the b quarks are so heavy. The v^2/c^2 terms should be relatively small, as should the strong coupling constant α_s evaluated at the b quark mass.

One can try to describe the Υ as a pair of heavy quarks bound in a potential well. Work is in progress on calculating the potential in lattice-QCD (Ref. 12). In the meantime, we use ideas from QCD to suggest the shape of the potential

$$V(r) = -\frac{4}{3}\frac{\alpha_s}{r} + kr$$

as a "Coulomb"term (corresponding to one gluon exchange) which dominates at short distances, plus a linear "confining"term (QCD string) which dominates at large distances. This type of potential was developed to describe the $c\bar{c}$ system (Ref. 13).

Two types of procedures have been used to deal with the r or Q^2 dependence of α_s, which to next-to-leading order[1] is

$$\alpha_s(Q^2) = \frac{1.51}{ln(Q^2/\Lambda^2_{\bar{M}S})} - 1.11\ \frac{ln(ln(Q^2/\Lambda^2_{\bar{M}S}))}{ln^2(Q^2/\Lambda^2_{\bar{M}S})} .$$

In the "Cornell" model, $\alpha_s \to \alpha_s(m_q^2)$: for a given m_q, α_s is a constant which is adjusted to fit the data. This effectively averages over the r dependence of α_s. Typically one needs an "effective"Λ of about 500 MeV to get a good fit.

[1]Evaluated for 4 quark flavors from Ref. 14.

However, because it is only "effective"one doesn't worry terribly much that other recent experiments indicate that the real Λ is more like 100-200 MeV. For QCD fans, this is rather unsatisfying, but this approach has the advantage of simplicity and thus relative ease of calculation. Much further work has been done in this framework (e.g. Ref. 15): incorporating relativistic correction (v^2/c^2) and spin-dependent terms, and calculating E1 and M1 transition rates.

In the second, more QCD-like approach used by Richardson (Ref. 16), the leading-order Q^2 dependence of α_s (the first term in the above α_s formula) is incorporated explicitly in $V(Q^2)$, which then gets Fourier transformed into V(r). Richardson formed a $V(Q^2)$ which interpolates smoothly between Coulomb and linear behavior. He starts with the Coulomb form $V(Q^2)$ = -4/3 α_s/Q^2 and replaces $ln(Q^2/\Lambda^2)$ by $ln(1 + Q^2/\Lambda^2)$ in the expression for α_s. He has only the one free parameter Λ which determines both short-range and long-range behavior. However his choice of interpolating form is in effect another degree of freedom. His fit to the ψ and Υ systems required $\Lambda \approx 400$ MeV.

Buchmüller, Grunberg and Tye (Ref. 17) include the next-to-leading order QCD corrections (second term in above formula for α_s) which are needed to make Λ well defined. They introduce one additional parameter ℓ, and the additional constraint that the long-range behavior of the potential agree with the meson Regge slope. They need $\Lambda_{\bar{M}S} = 500$ MeV. Some later models along this line (Ref. 18) can fit the data with smaller $\Lambda_{\bar{M}S}$, but only at the expense of introducing more parameters.

The difficulties of calculating ln with this complicated α_s dependence means that not much work has been done on spin-dependence or relativistic corrections. An exception is the recent paper by Bander, Silverman, Klima and Maor (Ref. 19), based on the Richardson potential. Here the relativistic effects require the introduction of a small-r cutoff parameter, and many of the results are sensitive to the value chosen.[1] They use Λ = 400-500 MeV.

[1]Relativistic effects also require a cutoff in the Cornell model (Ref. 15).

I find it rather worrisome that Λ seems to stick at 400-500 MeV. In my search for a model which can describe all the data with one consistent set of parameters, I have settled for this talk on the model of Gupta, Radford and Repko (Ref. 20). They use $\alpha_s(m_q^2)$, but have calculated 2 gluon exchange corrections to the Coulomb part of the potential, to which they add a linear confining term. They can fit the data with $\Lambda_{\overline{MS}} \sim 100$ MeV, as I will show in the course of this talk. I hope the discussion above of various other models will help guide the reader to his own choice.

The models have parameters corresponding to Λ, the quark mass m_q, perhaps the string constant k, and often a few more for technical reasons. These parameters are then adjusted until the 1S, 2S, and 3S energy levels of the potential V match the Υ, Υ′, and Υ″ masses:

$$M_{nS}(Q\bar{Q}) = 2m_Q + E_{nS}(m_Q, V).$$

These masses constrain the static potential V(r) in the range $0.2 < r < 1.0$ Fermi, which corresponds to the average radii of the states (Figure 2).

All models which fit the data agree in that range, although they may disagree strongly outside it. In particular, the model of Martin ($V(r) = A + Br^{0.1}$, Ref. 21) which has nothing to do with QCD, differs from the more standard QCD-inspired models for $r < 0.1$ Fermi.

This suggests the small-r region as a useful testing-ground for the importance (or lack thereof) of QCD in describing bound $q\bar{q}$ states. What can we measure that is sensitive to $r < 0.1$ Fermi? One might hope that probing the wave function at short distances would tell us something about the potential there:

$$\Psi(0) \iff V(0) \quad ?$$

even though the normalization of the wave function is affected by all r. Processes like $\Upsilon \to \ell^+\ell^-$ and $\Upsilon \to ggg$, which involve $b\bar{b}$ annihilation, are proportional to $|\Psi(0)|^2$ because the quarks must come together in order to annihilate (Fig. 3).

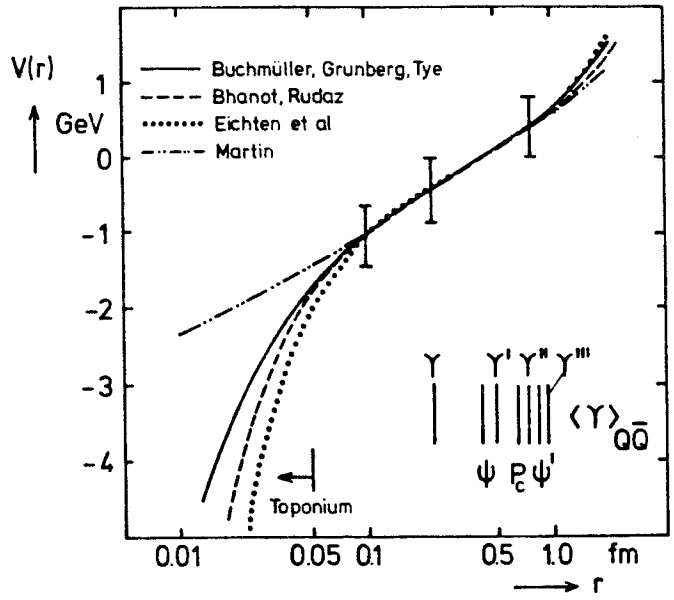

Figure 2. The static potential V(r) for various models (from Ref. 17). The potentials have been shifted to agree at r=0.5. — - - Martin potential, Ref. 21; —— Buchmüller *et. al.*, Ref. 17; - - Bhanot and Rudaz, Phys. Lett. 78B (1978) p. 119; ... Cornell potential, Ref. 13.

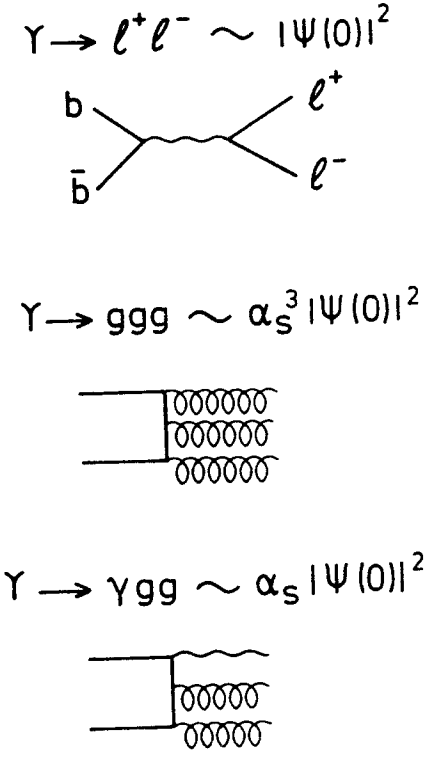

Figure 3. Decays of Υ.

$\Upsilon \to \ell^+\ell^-$

The rate for $\Upsilon \to \ell^+\ell^-$ in 0^{th} order in α_s is given by the Van Royen-Weisskopf formula (Ref. 22):

$$\Gamma^0_{ee} = \frac{16\pi\alpha^2_{em}e_q^2}{M^2_\Upsilon} |\Psi(0)|^2.$$

In any perturbation theory calculation, one must calculate, or at least be able to estimate the magnitude of the corrections in order to know whether to take the calculation seriously. For $\Upsilon \to \ell^+\ell^-$, the α_s term has been calculated explicitly (Ref. 23,24), but the α_s^2 and the relativistic correction are unknown. The best we can do at the moment (as suggested in Ref. 17) is to estimate the uncertainty due to these terms by giving the α_s^2 term the same coefficient as the α_s term, and the relativistic correction the magnitude of v^2/c^2.

$$\begin{aligned}\Gamma_{ee} &= \Gamma^0_{ee} \{1 - \frac{16\pi}{3}\alpha_s + O(\alpha_s^2) + O(v^2/c^2)\} \\ &= \Gamma^0_{ee} \{1 - 1.7\alpha_s \pm 1.7\alpha_s^2 \pm v^2/c^2\} \\ &= \Gamma^0_{ee} \{1 - .25 \pm .04 \pm .10\}.\end{aligned}$$

This gives us $\sim$ 20% uncertainty in the calculation of Γ_{ee}, in addition to any uncertainly in $\Psi(0)$ or in α_s[1]. This is rather much to handle at once. We can get on somewhat firmer ground by taking the ratio

$$\frac{\Gamma_{ee}(nS)}{\Gamma_{ee}(1S)} = \frac{|\Psi(0)|^2(ns) \quad \{1 - \ldots\}}{|\Psi(0)|^2(1s) \quad \{1 - \ldots\}}$$

(where the $\{1 - \ldots\}$ is to represent the corrections term, as above. The $\{1 - \ldots\}$ doesn't cancel completely because the radiative correction might depend on n, but the α_s terms are the same, so we can expect < 10% uncertainty for the ratio.

[1]Here I have used $\Lambda_{\overline{MS}} = 100MeV \to \alpha_s(.71M_\Upsilon) = 0.146$. The $0.71M_\Upsilon$ is the scale chosen in Ref. 40 for $e^+e^- \to hadrons$, and is also appropriate for Γ_{ee} (Brodsky, private communication). See also discussion on scale ambiguities in next section of this talk.

Measurements of Γ_{ee} are made from the area of the resonance peak in the total cross section (Figure 1):

$$\frac{M^2}{6\pi^2}\int \sigma_{had}\, dE \;=\; \Gamma_{ee}\;\frac{\Gamma_{had}}{\Gamma_{tot}} \;=\; \Gamma_{ee}\;\;(1-3B_{\ell\ell})\,.$$

Since $B_{\ell\ell}$ is small, its uncertainty has a small effect on that of Γ_{ee}.

The experimental results are summarized in Table 2a and compared with models in Table 2b. The experimental errors for the ratios $\Gamma_{ee}(nS)/\Gamma_{ee}(1S)$ are comparable to the caclulation errors discussed above, and the agreement is satisfactory within those errors. However the potentials which differ at r=0 turn out not to differ much in the ratio. For Γ_{ee}(1S), the Martin potential is different, and does not agree as well with the data. This looks promising, but before we get too excited, the α_s^2 term needs to be properly calculated. Also, one needs to study how well the model parameters are determined by the fit to the Υ masses, and how uncertainty in these parameters propagates into an uncertainty in the predicted Γ_{ee}.

Table 2a. Measurements of Γ_{ee} (in keV)

1S	1.46 ± 0.15*	PLUTO	Ref. 25
	1.08 ± 0.25	DESY-Heidelberg	Ref. 26
	$1.23 \pm 0.08 \pm 0.12$	DASP II	Ref. 27
	$1.13 \pm 0.09 \pm 0.08$	LENA	Ref. 28
	$1.30 \pm 0.05 \pm 0.08$	CLEO	Ref. 29
	$1.15 \pm 0.05 \pm 0.10$	CUSB	Ref. 7
	1.25 ± 0.07	average	
2S	$0.56 \pm 0.07 \pm 0.05$*	LENA	Ref. 30
	0.39 ± 0.17*	DESY-Heidelberg	Ref. 26
	$0.58 \pm 0.12 \pm 0.06$*	DASP II	Ref. 27
	$0.56 \pm 0.03 \pm 0.05$	CUSB	Ref. 7
	$0.52 \pm 0.03 \pm 0.04$	CLEO	Ref. 29
	0.53 ± 0.04	average	
3S	$0.39 \pm 0.02 \pm 0.03$	CUSB	Ref. 7
	$0.42 \pm 0.04 \pm 0.03$	CLEO	Ref. 29
	0.40 ± 0.04	average	
4S	$0.28 \pm 0.04 \pm ?$	CUSB (prel.)	Ref. 7
	$0.19 \pm 0.01 \pm 0.04$	CLEO (prel.)	Ref. 6
	0.23 ± 0.04	average	
5S	$0.37 \pm 0.06 \pm ?$	CUSB (prel.)	Ref. 7
	$0.22 \pm 0.05 \pm 0.07$	CLEO (prel.)	Ref. 6
	0.29 ± 0.08	average	

* The published value assumed $\Gamma_{had} = \Gamma_{tot}$. I have corrected it using $B_{\ell\ell}(1S) = 3.0\%$, $B_{\ell\ell}(2S) = 1.8\%$.

Table 2b. Comparison of Experiment and Models: Γ_{ee}

	experiment	model Gupta (Ref. 20) ($\Lambda = 100$ MeV)	Martin (Ref. 21) ($A + Br^{0.1}$)
1S	1.25 ± 0.07	1.29 ± 0.26	0.80 ± 0.16‡
			0.57 ± 0.07*
2S/1S	0.42 ± 0.04	0.48 ± 0.05	0.51 ± 0.05
3S/1S	0.32 ± 0.04	0.36 ± 0.04	0.35 ± 0.04
4S/1S	0.18 ± 0.03		0.27 ± 0.03
5S/1S	0.23 ± 0.06		0.21 ± 0.02

‡ corrected by 0.75 for 1*st* order. * scaled from measured $\Gamma_{ee}(\psi)$

$\Upsilon \to ggg$

The width of the Υ is almost entirely due to its three gluon decay. However, since its width is narrower than the resolution of the storage ring, we cannot measure it directly. Instead, we measure the Υ branching ratio to lepton pairs

$$B_{\ell\ell} = B_{\mu\mu} = B_{ee} = B_{\tau\tau}$$

assuming lepton universality. This, together with our measured Γ_{ee}, gives us the total width indirectly via

$$\Gamma_{tot} = \frac{\Gamma_{ee}}{B_{\ell\ell}}.$$

Thus we see that $B_{\ell\ell}$ is the more fundamental experimental quantity.

Measurement of $B_{\ell\ell}$ is difficult because it is small. The standard method is to compare $e^+e^- \to \mu^+\mu^-$ on and off resonance. The $e^+e^- \to \mu^+\mu^-$ cross section is small everywhere, requiring long run periods over which one must make sure one has no change in efficiency. This efficiency is usually not known *apriori*, but is derived by normalizing the off-resonance result to the QED $e^+e^- \to \mu^+\mu^-$ cross section. Data from CLEO are shown in Figure 4, and results from all experiments are accumulated in Table 3.

Table 3. Measurements of $B_{\ell\ell}$ (in %)

	$\Upsilon(1S)$		
$\Upsilon \to \mu\mu$	2.2 ± 2.0	PLUTO	Ref. 25
$\Upsilon \to ee$	5.1 ± 3.0	PLUTO	Ref. 31
$\Upsilon \to \mu\mu$	$3.8 \pm 1.5 \pm 0.2$	LENA	Ref. 28
$\Upsilon \to \mu\mu$	$3.2 \pm 1.3 \pm 0.3$	DASP II	Ref. 27
$\Upsilon \to \mu\mu$	$2.7 \pm 0.3 \pm 0.3$	CLEO	Ref. 32
$\Upsilon' \to \pi\pi\Upsilon, \Upsilon \to ee$	3.9 ± 1.1	CLEO	Ref. 33
$\Upsilon \to \tau\tau$	$3.4 \pm 0.4 \pm 0.4$	CLEO	Ref. 34
$\Upsilon \to \mu\mu$	$2.7 \pm 0.3 \pm 0.3$	CUSB	Ref. 35
$\Upsilon' \to \pi\pi\Upsilon, \Upsilon \to ee$	$2.8 \pm 0.4 \pm 0.3$	ARGUS (prel.)	Ref. 36
	$\overline{3.0 \pm 0.3}$	average	
	$\Upsilon'(2S)$		
$\Upsilon' \to \mu\mu$	$1.8 \pm 0.8 \pm 0.5$	CLEO	Ref. 37
$\Upsilon' \to \tau\tau$	$1.7 \pm 1.5 \pm 0.6$	CLEO	Ref. 37
$\Upsilon' \to \mu\mu$	$1.9 \pm 0.3 \pm 0.5^*$	CUSB	Ref. 35
$\Upsilon' \to \mu\mu$	$1.6 \pm 0.6 \pm 0.5^*$	ARGUS (prel.)	Ref. 38
	$\overline{1.8 \pm 0.6}$	average	
	$\Upsilon''(3S)$		
$\Upsilon'' \to \mu\mu$	$3.3 \pm 1.3 \pm 0.7$	CLEO	Ref. 32

* scaled to 1S value

Instead of subtracting the continuum, one can select Υ from $\Upsilon' \to \pi\pi\Upsilon$, and measure the fraction that decay to leptons:

$$B_{ee} = \frac{\Upsilon' \to \pi\pi\Upsilon, \Upsilon \to ee}{\Upsilon' \to \pi\pi\Upsilon, \Upsilon \to all}.$$

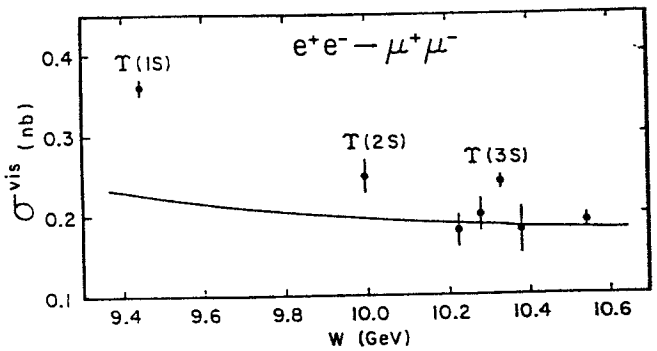

Figure 4. The $e^+e^- \to \mu^+\mu^-$ cross-section (CLEO data from Ref. 32).

This technique requires good resolution to select the Υ in the missing mass against π pairs independent of the type of Υ decay. Results from CLEO and ARGUS are included in Table 3.

On the theory side, $B_{\ell\ell}$ also starts with an advantage. In the ratio $B_{\ell\ell}$ the $|\Psi(0)|^2$ dependence divides out, leaving a very strong dependence on α_s:

$$B_{\ell\ell} \approx \frac{\Upsilon \to \ell\ell}{\Upsilon \to ggg} \propto \frac{1}{\alpha_s^3}.$$

This means that even a poor measurement of $B_{\ell\ell}$ should give a good measurement of α_s!

Correcting for all decay modes $\Upsilon \to ggg + q\bar{q} + \gamma gg + ee + \mu\mu + \tau\tau$ (see e.g. Ref. 39) and using $B_{\ell\ell} = (3.0 \pm 0.3)\%$, we have

$$\frac{\Gamma_{ggg}}{\Gamma_{ee}} = \frac{1 - 7.3B_{\ell\ell}}{B_{\ell\ell}} = 26 \pm 3.$$

To 0^{th} order in QCD (see e.g. Ref. 39)

$$\alpha_s = 0.0558 \sqrt[3]{\frac{\Gamma_{ggg}}{\Gamma_{ee}}} = 0.165 \pm 0.005.$$

The 1^{st} order correction to Γ_{ggg} has been calculated (Ref. 39), leading to

$$\alpha_s(M) = \frac{0.165}{\sqrt[3]{1 + C(M)\alpha_s(M)}}.$$

If one chooses M = $0.48M_\Upsilon$, the correction vanishes (C($0.48M_\Upsilon$)=0.0).

What does it mean that we can *choose* M? The coefficients of α_s^n(M) correction terms depend on the choice of M. If one could calculate to all orders, the change in the coefficients of the various orders would compensate each other in such a way as to give the same result for Γ_{ggg}. But in a 1^{st} order calculation, one can get any coefficient one wants by changing M. One has usually relied on a *reasonableness* in the choice of M to make sense of 1^{st} order calculations; $M \approx .5M_\Upsilon \approx m_b$ seemed reasonable for Υ decays. Changing to $M = M_\Upsilon$ (C(M_Υ)=2.9) would change the result from

$$\alpha_s(.48M_\Upsilon) = 0.165 \quad \text{to} \quad \alpha_s(M_\Upsilon) = 0.147.$$

However, Brodsky, LePage and Mackenzie have studied the problem of scale ambiguities in QCD (Ref. 40) and conclude that one should use $M = 0.157M_\Upsilon$ in this process. Also, C($0.157M_\Upsilon$) = -4.5, which gives the above equation for α_s a pole at α_s=0.22, and no reasonable solution. It seems that the process $\Upsilon \to ggg$ cannot be calculated in QCD using present techniques. Since it would be such a good way to measure α_s, let us hope that a way will be found to get theory in the same realm as experiment, where the measurements of $B_{\ell\ell}$ are now good to 10%.

$$\underline{\Upsilon \to \gamma gg}$$

One way out of this theoretical nightmare might be

$$\frac{\Upsilon \to \gamma + hadrons}{\Upsilon \to hadrons} \approx \frac{\Upsilon \to \gamma gg}{\Upsilon \to ggg} \propto \frac{1}{\alpha_s}.$$

Here the troublesome part of the QCD diagram divides out so that the 1^{st} order correction is small, even for M=$0.157M_\Upsilon$ (Ref. 40):

$$\frac{\Upsilon \to \gamma gg}{\Upsilon \to ggg} = \frac{0.58\%}{\alpha_s}\{1 + 0.72\alpha_s\}.$$

Results on the branching ratio of $\Upsilon \to \gamma gg$ are $(3.0 \pm 0.6)\%$ from CUSB (Ref. 41) and $(2.0 \pm 0.3 \pm 0.3)\%$ from CLEO (preliminary, Ref. 42). The average value $(2.5 \pm 0.4)\%$ gives

$$\frac{\Upsilon \to \gamma gg}{\Upsilon \to ggg} = (3.2 \pm 0.5)\%$$

and

$$\alpha_s(0.157M_\Upsilon) = 0.21 \pm 0.03, \quad \Lambda_{\overline{MS}} = 93 \pm 45 MeV$$

which is in agreement with the $\Lambda_{\overline{MS}}$ = 100 Mev used by Gupta *et. al.* in their potential. Here a certain caution is recommended, since this measurement is experimentally difficult. One must reliably separate γ's from the much larger number of π^0's. The direct-γ to π^0 ratio is better at higher γ energy; one relies on the theoretical shape of the spectrum to tell us that there are few direct

γ's at lower energies. We hope that more data will bring confirmation of this encouraging result.

We conclude at this point that the potential model can describe the $^3S_1$ Υ states reasonably well, and we now turn to the ^3P_j states for tests of the spin-dependence of the potential.

2. χ_b States

The χ_b states are produced in radiative decays of the Υ's:

$$\Upsilon' \rightarrow \gamma\chi_b \quad \text{and} \quad \Upsilon'' \rightarrow \gamma\chi_b', \gamma\chi_b.$$

They are ^3P_j $b\bar{b}$ states with the same total quark spin S=1 as the $^3S_1$ Υ states, but the quarks have relative orbital angular momentum L=1 instead of L=0. The three different possible relative orientations of $\vec{S}$ and $\vec{L}$ give J=0,1,2 states. The different strengths for the $L \cdot S$ interaction cause different masses for the $^3P_0$, $^3P_1$, and $^3P_2$ states. This means that measurement of the χ_b masses allows us to probe the spin structure of the potential. If the $^1S_0$ η_b and the $^1P_1$ are found, they will provide tests of the $S \cdot S$ interaction. The various states are shown schematically in Figure 5, and the possible transitions between them are sketched in Figure 6.

Measurements of χ_b', χ_b

Observation of the ^3P_j states occurs in two types of analyses:

a) The inclusive photon spectum from $\Upsilon' \rightarrow \gamma + hadrons$, where one expects to see three photon lines from $\Upsilon' \rightarrow \gamma\chi_b$ transitions to the J=2,1,0 χ_b states. Two additional lines corresponding to the $\chi_b \rightarrow \gamma\Upsilon$ decays of the J=2,1 states usually appear merged into one broader line. The corresponding decay of the J=0 state is expected to be too small to observe.

b) The exclusive reaction $\Upsilon' \rightarrow \gamma\chi_b$, $\chi_b \rightarrow \gamma\Upsilon$, $\Upsilon \rightarrow \ell\ell$ where one observes the final state $\gamma\gamma\ell\ell$. Since one expects the Υ' - χ_b mass difference to

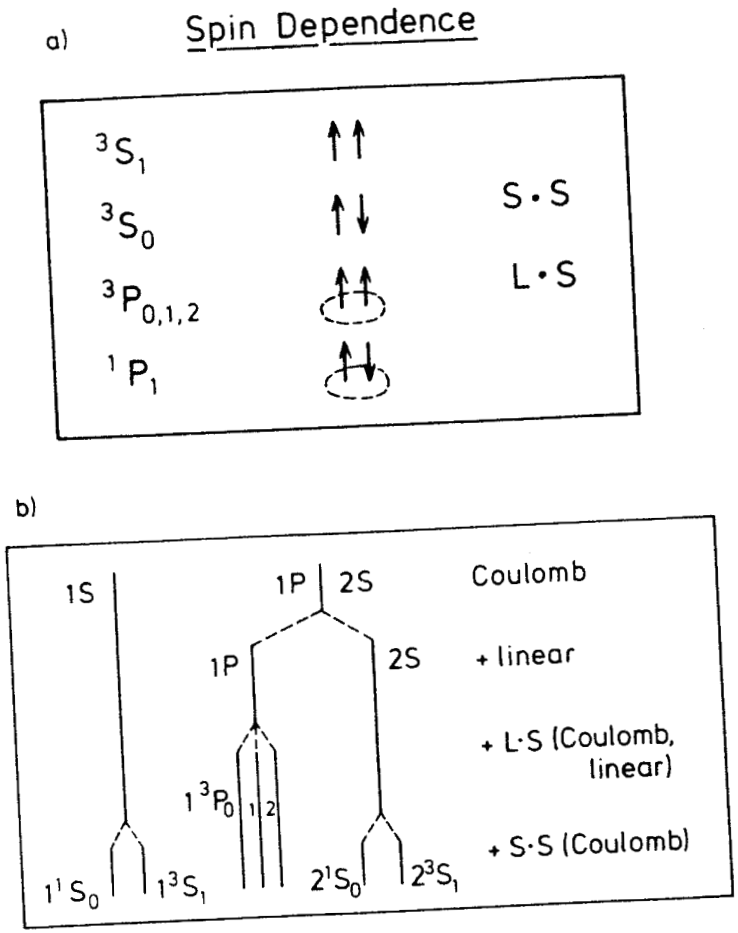

Figure 5. a) Quark spin and angular momentum states; and b) Splitting of states by various interaction terms.

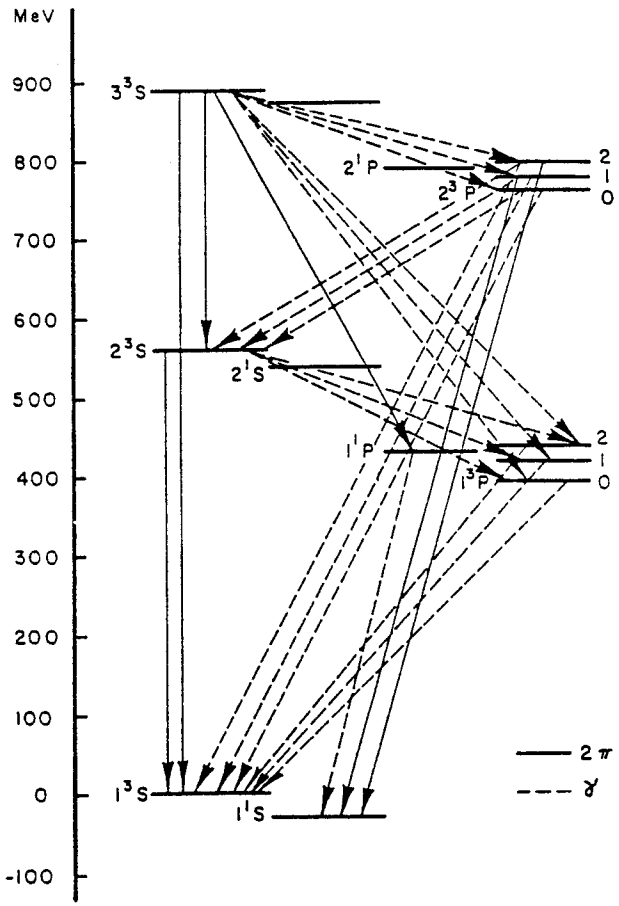

Figure 6. Transitions between $b\bar{b}$ states.
Vertical axis is mass relative to the Υ in MeV.

be smaller than the χ_b - Υ, one chooses the lower energy photon as the primary photon in each event.

In general the inclusive analysis has the advantage of higher statistics; the exclusive of lower background. The results from all experiments are discussed below, and summarized in Tables 4a and 4b.

Table 4a. CUSB Measurements of χ_b', χ_b States.

	χ_b' Inclusive	χ_b' Exclusive	χ_b Inclusive	χ_b Exclusive
σ_E(100 MeV)	~ 8.7 MeV	~ 6.5 MeV	6.4 MeV	5.3 MeV
σ_E(130 MeV)			7.8 MeV	
eff.(100 MeV)	~ 17%			
eff.(80-500)			13%	
# hadronic events observed	65K		230K	
# T″ decays, # T′ decays observed	37K		153K	
Photon Energies in MeV				
E_1	$84 \pm 2 \pm 4$	84 ± 3*	$108.2 \pm 0.3 \pm 2$	$107.0^{+2.0}_{-2.5} \pm 2$
E_2	$99 \pm 3 \pm 4$	99 ± 2*	$128.1 \pm 0.4 \pm 3$	$128.0 \pm 1.5 \pm 2$
E_3	$117 \pm 5 \pm 4$		$149.4 \pm 0.7 \pm 5$	
E_{cog}	93 ± 5		119 ± 3	
Statistical significance				
lines 1+2+3	11σ		9.6σ	
line 1			4.4σ	2.4σ
line 2			4.2σ	4.0σ
line 3			2.5σ	
Branching ratios in %				
lines 1+2+3	$34 \pm 3 \pm 3$		$15.5 \pm 2.5^{+5}_{-2}$	
line 1			6.1 ± 1.4	
line 2			5.9 ± 1.4	
line 3			3.5 ± 1.4	

* Errors do not include position/area correlations

Table 4b. Crystal Ball, CLEO, and ARGUS Measurements of χ_b States. Photon Energies in MeV

	Crystal Ball (prel.) Inclusive	Crystal Ball (prel.) Exclusive	CLEO Inclusive	ARGUS (prel.) Inclusive
σ_E(100 MeV)	$\sim$ 4.6 MeV		3.4 MeV	2.3 MeV
σ_E(130 MeV)	$\sim$ 5.6 MeV		4.4 MeV	2.1 MeV
eff.(108 MeV)			2.5%	0.23%
eff.(129 MeV)	$\}\sim 17\%$		3.2%	0.37%
eff.(155 MeV)			3.6%	0.51%
# hadronic events observed	253K	338K	220K	285K
# Υ' decays observed	124K	166K	125K	140K
Photon Energies in MeV				
E_1	$108.2 \pm 0.7 \pm 4$	$105.6 \pm 1.4 \pm 2$	$109.5 \pm .7 \pm 1$	$109.0 \pm 1.0 \pm 1$
E_2	$127.1 \pm 0.8 \pm 4$	$131.4 \pm 1.5 \pm 2$	$129.0 \pm .8 \pm 1$	$129.8 \pm 0.8 \pm 1$
E_3	$160.0 \pm 2.4 \pm 6$		$(158 \pm 7 \pm 1)^*$	$147.2 \pm 1.4 \pm 1$
E_{cog}	120 ± 5		121 ± 2	120 ± 2
Statistical significance				
line 1	8.6σ	7.9σ	5.7σ	3.0σ
line 1	8.3σ	7.6σ	4.7σ	4.0σ
line 1	3.9σ		$< 2\sigma$	2.2σ
Branching ratios in %				
line 1	$6.0 \pm 0.7 \pm 0.9$		$10 \pm 2 \pm 2$	$9 \pm 3 \pm 1$
line 2	$6.6 \pm 0.8 \pm 1.0$		$8 \pm 2 \pm 2$	$9 \pm 2 \pm 1$
line 3	$2.6 \pm 0.7 \pm 0.8$		< 8	$4 \pm 2 \pm 1$

* This line is not needed in the fit.

The first $b\bar{b}$ ^3P_j states were seen by CUSB in Υ'' decays $\Upsilon'' \to \chi_b'$ (Ref. 44). The CUSB detector, shown in Fig. 7, measures photon energies with 8 radiation lengths of NaI blocks followed by 7 radiation lengths of lead glass. The CUSB group observed a broad enhancement in the Υ'' inclusive photon spectrum at an average energy of 98 MeV (Fig. 8). This enhancement could not be fit by a single line; two lines gave a reasonable fit; three were preferred, and also expected, corresponding to the $^3P_2$, $^3P_1$, and $^3P_0$. The three line fit gave photon energies of 84, 99 and 117 MeV, and relative intensities in agreement with the

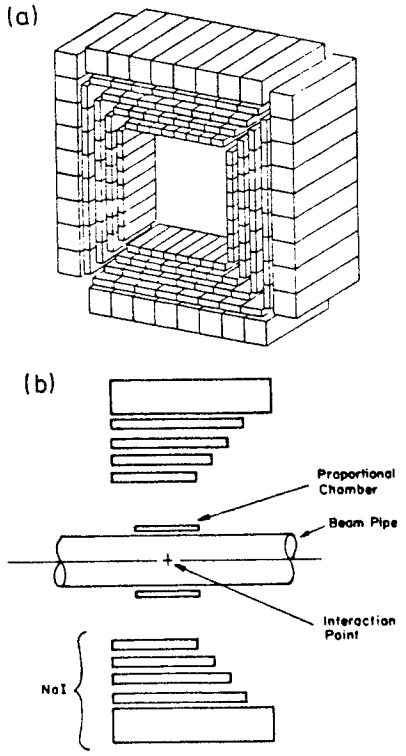

Figure 7. CUSB detector.
a) Isometric view of crystal array. b) Side view.

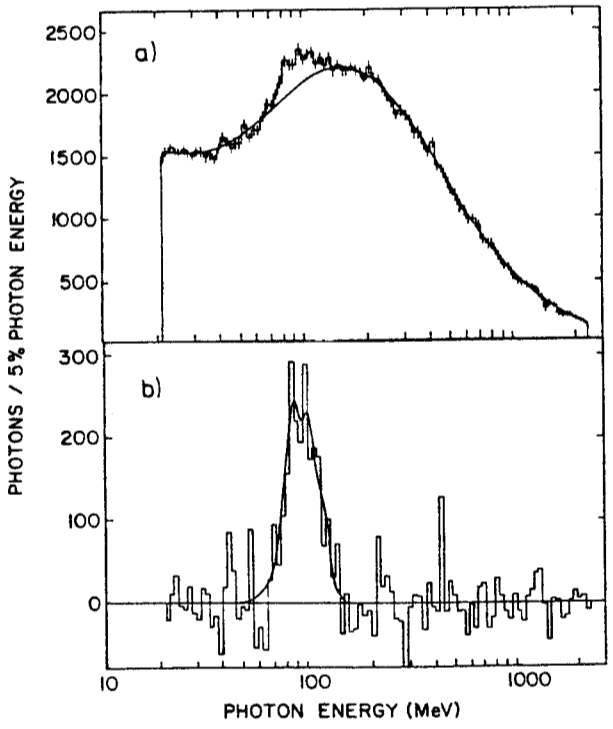

Figure 8. a) Observed inclusive photon spectrum $\Upsilon'' \to \gamma + hadrons$.
b) Background subracted.
CUSB data from Ref. **44**.

expected 2J+1 ratios. However the errors on the intensities are large, as are the correlations between the positions and intensities of the various lines. The result for all three lines added together should be more reliable. The center of gravity E_{cog} calculated from the fitted line energies is 93 MeV. I interpret the 5 MeV difference to the average energy of the "broad enhancement" to be indicative of the systematic uncertainty. The lower energy photon spectrum from the CUSB exclusive $\Upsilon'' \to \gamma\gamma\ell\ell$ analysis is shown in Figure 9a. Fitting this spectrum with two lines gives a good fit and energies in agreement with the first two lines in the inclusive spectrum.

Compared to $\Upsilon'' \to \chi_b'$, $\Upsilon' \to \chi_b$ is expected to have the advantage that the splitting is larger, but the branching ratios are smaller.

For their Υ' run, the CUSB group improved their photon resolution by removing the strip chambers[1] between the layers of NaI and tightening the photon selection cuts (Ref. 45). The Υ' inclusive photon spectrum is shown in Figure 10. The primary lines appear almost resolved around 125 MeV, and the $\chi_b \to \gamma\Upsilon$ photons are seen as one peak at $\sim$ 427 MeV. A three-line fit to the 125 MeV region is prefered over a one- or two-line fit and gives energies of 108, 128, and 149 MeV. The exclusive spectrum, shown in Figure 9b, shows two peaks in good agreement with the first two seen in the inclusive spectrum.

In the meantime, in order to study the Υ system, the Crystal Ball detector was moved from SPEAR to DORIS. The Crystal Ball (Fig. 11) is a spherical shell of NaI, 16 radiation lengths thick, segmented into 720[2] triangular crystals pointing towards the interaction region. Data equivalent to 200K produced $\Upsilon'(2S)$ has been accumulated; the analysis on the first 3/4 has been completed. Figure 12 shows a typical hadronic event in the Crystal Ball. The Υ' inclusive

[1] The chambers degrade the energy resolution because shower energy deposited in their material is not measured.

[2] Minus a few to make room for the beam pipe.

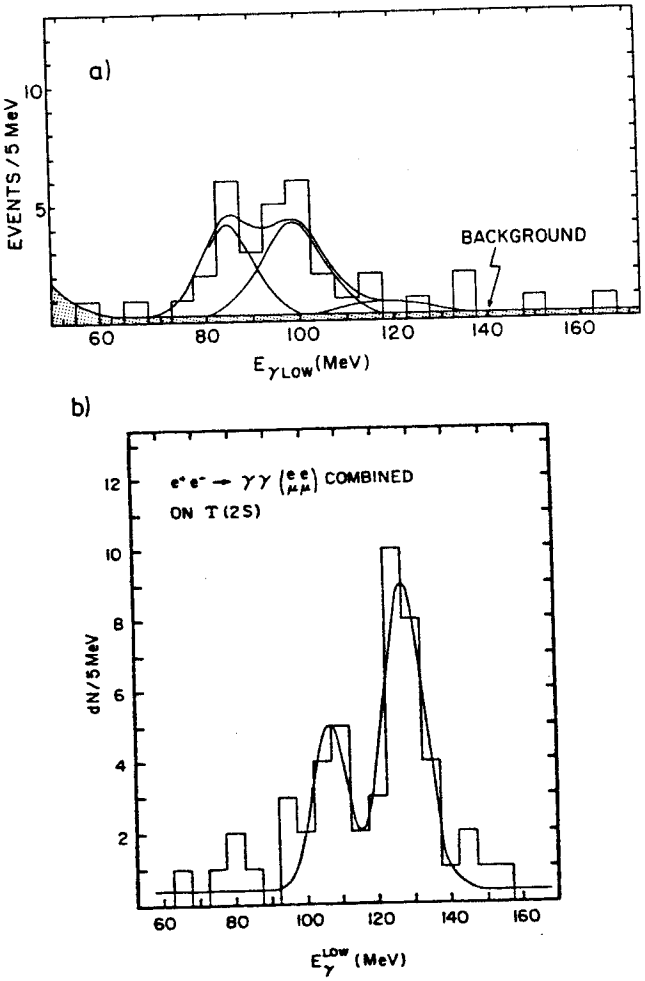

Figure 9. a) Low energy photon spectrum from $\Upsilon'' \to \gamma\gamma\ell\ell$, and
b) from $\Upsilon' \to \gamma\gamma\ell\ell$.
CUSB data from Ref. 44, 45.

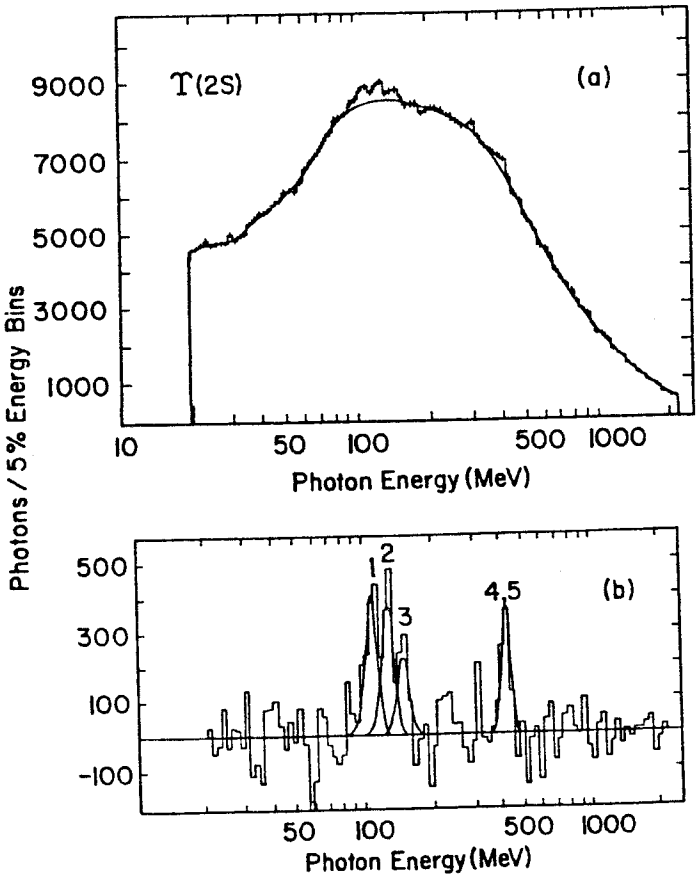

Figure 10. a) Observed inclusive photon spectrum $\Upsilon' \to \gamma + hadrons$.
b) Background subtracted.
CUSB data from Ref. 45.

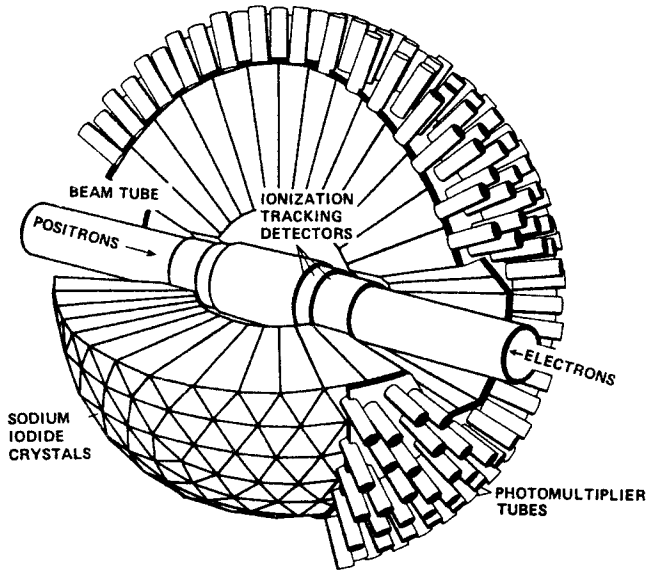

Figure 11. Crystal Ball Detector

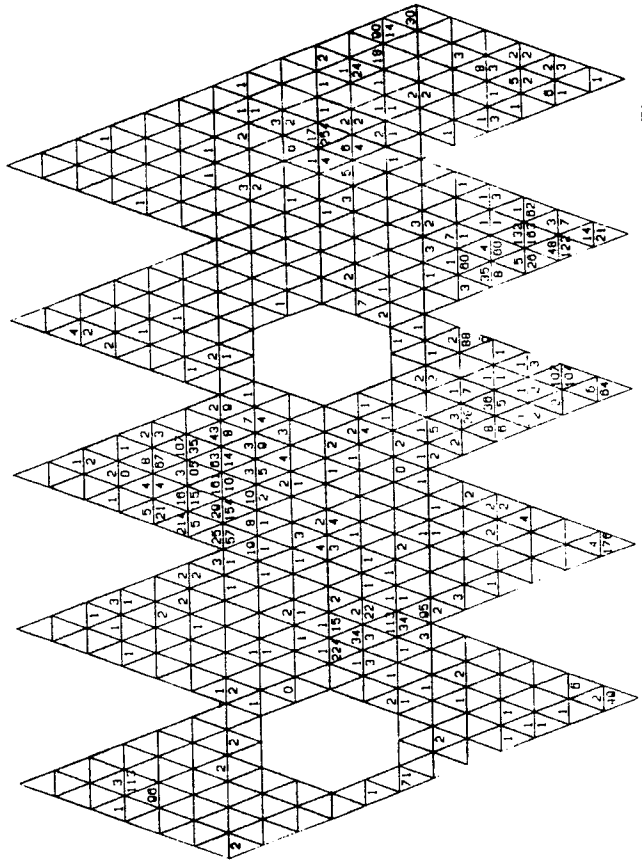

Figure 12. A typical hadronic event as seen in the Crystal Ball. The crystals of the sphere are shown in a flat projection. The numbers are the detected energies per crystal in MeV.

photon spectrum is shown in Figure 13. Three clear peaks are seen at 108, 127 and 160 MeV. At 208 MeV another peak is evident, which is due to misidentified minimum ionizing charged particles. Normally, charged particles make hits in the three double layers of proportional tube chambers which surround the beam pipe, and can be removed from the photon sample. However the magic gas in these chambers succumbed to the higher backgrounds at the Υ', resulting in poor chamber efficiency. The photon spectrum was fit with 3 Gaussians for the primary lines, a charged-particle spectrum with variable normalization, and two Doppler-broadened lines for the merged secondary-photon peaks seen near 420 MeV. The proximity of the charged-particle peak to the 160 MeV line produces a larger systematic error there. Nevertheless, even this line has a statistical significance of nearly 4σ, and all three primary lines are well resolved.

In its exclusive analysis (Fig. 14) the Crystal Ball group sees two well-resolved lines at 106 and 131 MeV. There are 67 events in the peaks, with practically no background. A spin analysis is in progress, which we hope will tell us if the first line is due to a spin 2 state, and the second to spin 1, as we expect from the potential model and from the example of the $c\bar{c}$ χ states.

The magnetic detectors CLEO and ARGUS can also measure photons with good resolution, in the rare cases where the photon converts into an e^+e^- pair before entering the main tracking chamber. A picture of such an event in the ARGUS detector is shown in Figure 15.

For its Υ' run, the CLEO group increased the amount of material before the main chamber to 0.15 radiation lengths to improve the conversion probability, and reduced the magnetic field to 3.5 kG to get better tracking efficiency for low momentum particles (Ref. 47). The inclusive converted photon spectrum is shown in Figure 16. Two peaks are evident, at 109 and 129 MeV. A third peak is not required by the data. If one is put into the fit, it comes out at 158 MeV and has less than 2σ significance.

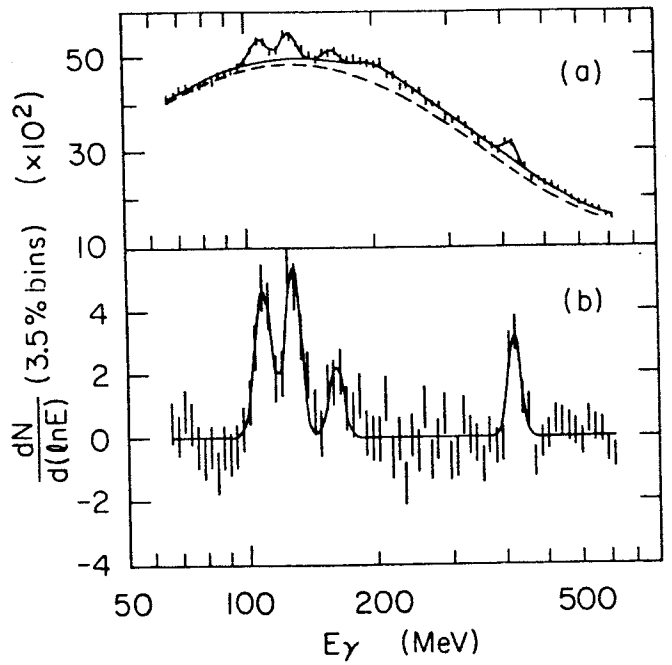

Figure 13. a) Observed inclusive photon spectrum $\Upsilon' \to \gamma + hadrons$.
b) Background subracted.
Crystal Ball data.

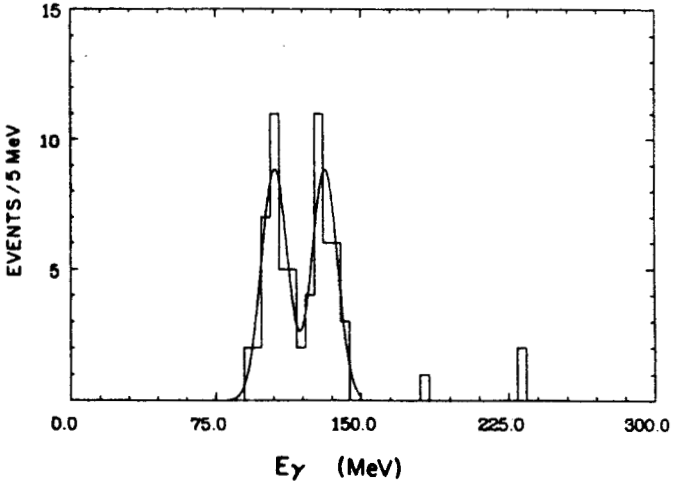

Figure 14. Low energy photon spectrum from $\Upsilon' \to \gamma\gamma\ell\ell$. Crystal Ball data.

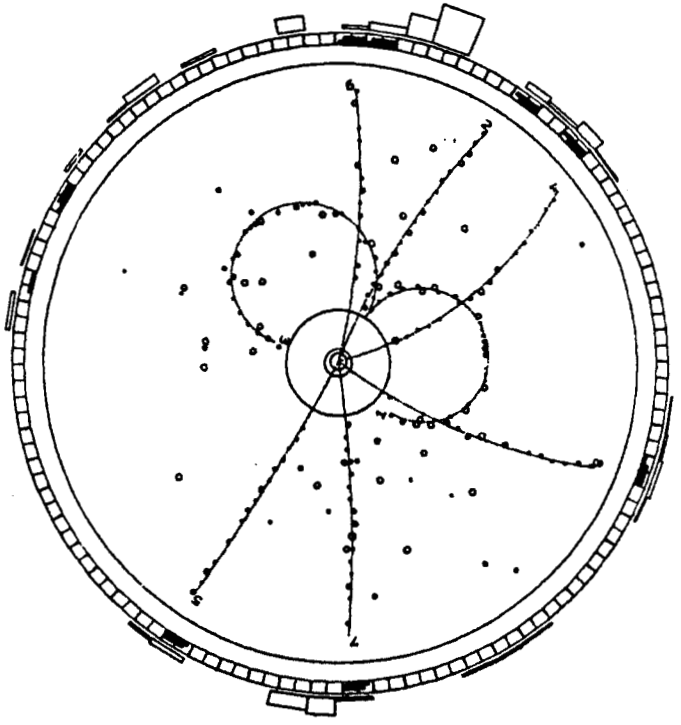

Figure 15. A converted photon in the ARGUS detector.

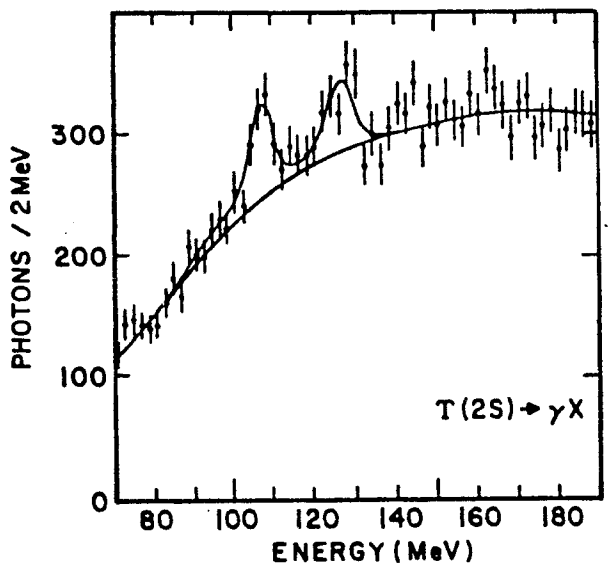

Figure 16. Observed converted photon spectrum $\Upsilon' \rightarrow \gamma + hadrons$; CLEO data from Reference 47.

The ARGUS detector has 0.035 radiation lengths of material before the main chamber, and a magnetic field of 8 kG. The ARGUS group has recently developed special software for efficiently tracking low momentum particles. The resulting converted photon spectrum is shown in Figure 17a (Ref. 38). The peaks at 109, 130 and 147 MeV are very well separated, but the statistical significance is low, especially for the third line at 2.2σ. Although the ARGUS energy resolution is very good, and the fit gives the errors on the peak positions as $\sim$ 1 MeV, the low statistical significance of the peaks gives another uncertainty which is not reflected in this fit error. This can be seen by comparing Figure 17a to Figure 17b, which is the same data sample before improved tracking. The fit to this older spectrum gave peaks with errors of 2 MeV at 112, 132, and 157 MeV with statistical significances 2.6, 4.4, and 2.5 σ. The first two lines are in good agreement with the newer result; the third is not. It seems to be a general problem with fits to peaks of low statistical significance: the uncertainty of the existence of the peak is not properly reflected in the uncertainty of the peak position.

Where Are the Peaks Really?

The χ_b results from all experiments are compared in Figure 18. The results for the first two lines agree very well, so that we can use the weighted averages of 109 ± 1 and 129 ± 1 MeV. The agreement on the third line is not so good. For now, I am forced to take as average a value which can be stretched to agree with all experiments: 154 ± 9 MeV. In view of the previous discussion on fit errors this is perhaps to be expected, since CUSB, CLEO, and ARGUS all observe the third line with low significance. The preliminary Crystal Ball result has a large systematic error; however this is still under intensive study and may improve. I have made a point of showing the plots from all experiments, to encourage the reader to form his own judgement of the situation.

Fortunately the position of the third line doesn't have much effect on the spin-weighted average, which becomes 121 ± 2 MeV. The center of gravity of

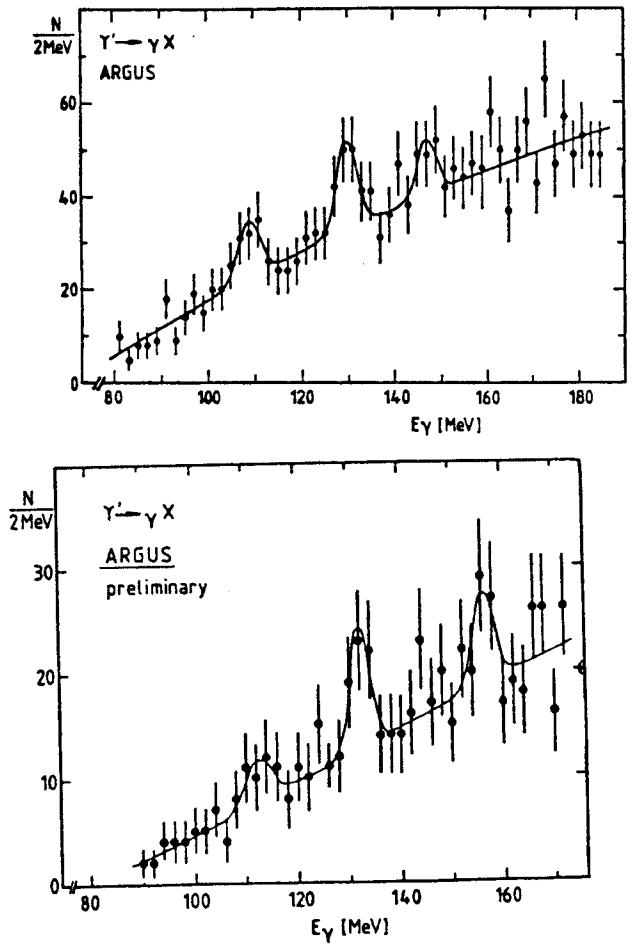

Figure 17. a) ARGUS converted photon spectrum, Summer 1984 status.
b) Same, Spring 1984 status.

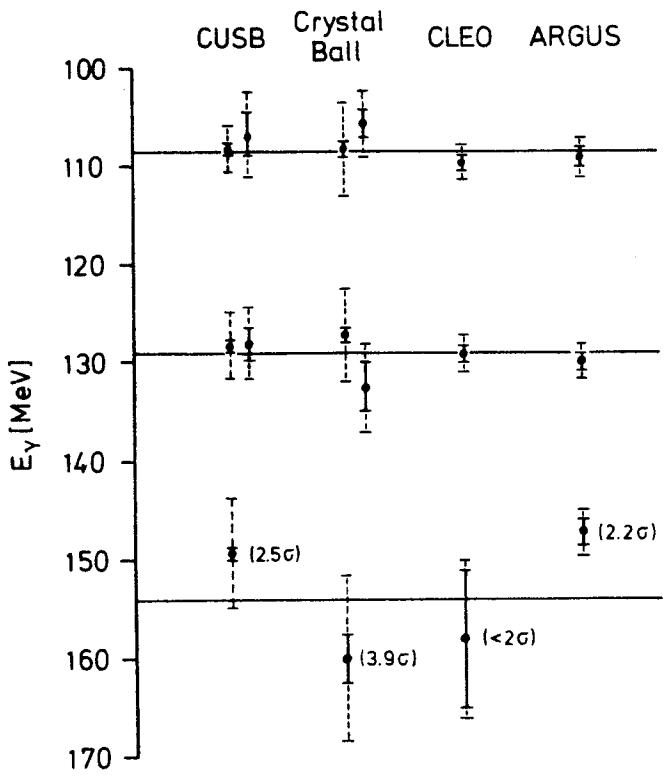

Figure 18. Comparison of Results on Photon Lines from $\Upsilon' \to \gamma\chi_b$.
The solid inner error bars are the statistical errors. The outer ones are the systematical errors, added linearly. The statistical significances of the third lines are given in parentheses.

the χ_b states is then at 9901 ± 2 MeV. The ratio of the splittings *is* strongly affected by the third line:

$$\frac{E_2 - E_1}{E_3 - E_2} \quad = \quad r \quad = \quad 0.8 \pm 0.3.$$

Spin Dependence in the Potential

Knowledge of the static potential V(r) is not sufficient to describe interactions involving spin. For that, one must know the Lorenz form of the potential. Then the spin-dependence can be expressed (see e.g. Ref. 15) in terms of derivatives of the vector, scalar, ... parts of the static potential $V(r) = V_V(r) + V_S(r) + \ldots$.

The Coulomb part is clearly vector particle (gluon) exchange. For the long-range part, we have no sure theoretical guidance. Eichten and Feinberg (Ref. 43) have deduced from general principles that there are 4 independent terms. This generality gives us too many parameters to work with, so we must try some reasonable assumptions and test them against the data. Four assumptions have been tried: a) vector, b) scalar, c) vector + scalar, and d) electric. The first turns out to fail to fit the data, so we reject it. The other three must be investigated further.

The dependence of the masses on the various parts of the potential can be visualized as in Figure 5. Without spin, the Coulomb term alone has the S and P states degenerate. The addition of the linear term separates the S and P states, as an effect of the different r-dependence of their wave functions. The $L \cdot S$ term, which involves both the Coulomb and linear terms, splits the ^3P_j states. The $^1P_1$ mass and the spin-weighted average of the ^3P_j masses are not affected by the $L \cdot S$ term. That means that the Υ' - χ_b mass difference is controlled by the linear part of the potential.

The data for the χ_b' and χ_b center-of-gravities are compared to some theories in Table 5. The QCD-like models give a good description. That of Martin gives too large a splitting. This is perhaps indicative of an improper balance between the long-range and short-range parts of the potential.

Table 5. $\chi_b - \Upsilon$ Mass Difference

	Data	Martin (Ref. 21)	Richardson (Ref. 16)	Gupta *et al.* (Ref. 20)
$\Upsilon' - \chi_b$	122 ± 2 MeV	164	119	113
$\Upsilon'' - \chi_b'$	94 ± 5 MeV	118	97	97

Early predictions for r led one to hope that this ratio could decide between electric confinement ($r \sim 1$, Ref. 43) and scalar confinement ($r \approx 0.45$, Ref. 15). However the newer calculation of Gutpa *et al.* gives $r = 0.68$ for scalar confinement. Bander, Siverman, Klima, and Maor (Ref. 19) have used a Richardson-type potential to calculate pure scalar ($r \approx 0.75$) and vector+scalar confinement ($r \approx 0.87$). This freedom in the calculations, combined with the present large experimental uncertainty, leaves all options open for now.

At this point I would like to remind you that the potential model is a *model*, which has parameters which need to be fit to the data. The proper question in such a case is not *"Did it predict the states?"* but *"Can it fit them?"* The fairest answer to the second question would require re-determining the parameters using the newest data. However, even without this, the agreement is quite good, as shown in Figure 19. In addition, I wish to require that the parameters which fit are also reasonable: i.e. the same value of $\Lambda_{\overline{MS}}$ should be used to calculate masses and decay rates, and it should also agree with the value obtained in other reactions like deep-inelastic scattering. This is satisfied by the model of Gupta *et al.*.

Conclusions

The potential model can fit the $b\bar{b}$ masses. This is made easier by present uncertainties in both theory and data.

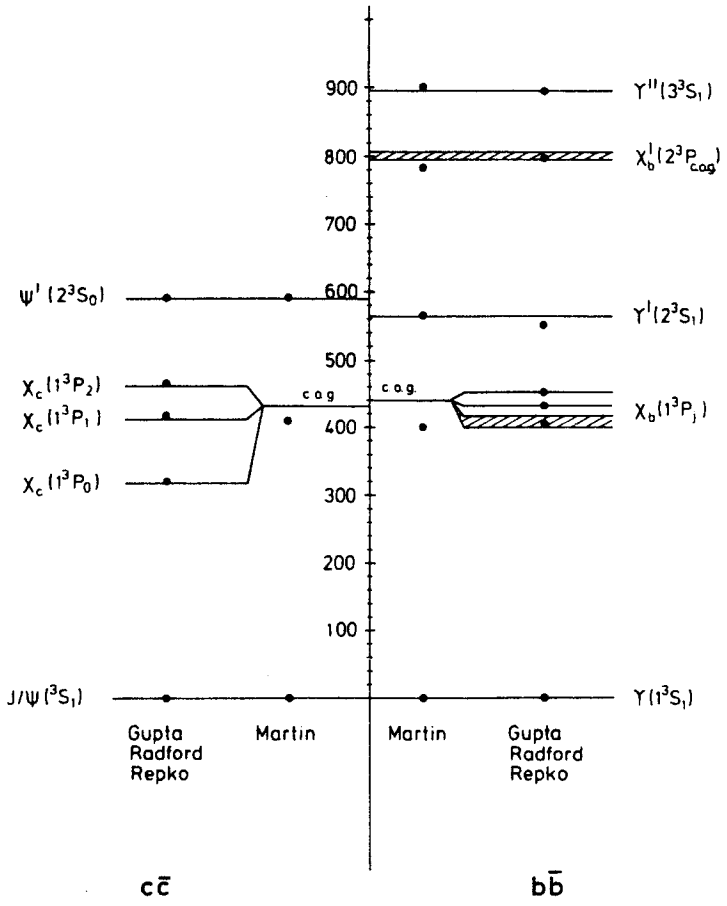

Figure 19. Comparison of theory with measured masses. Vertical axis is mass above ground state in MeV.

A reasonable model which was developed for $c\bar{c}$ can also fit $b\bar{b}$. It could have been otherwise – the model doesn't have *that* many parameters: It couldn't describe the wrong η_c (but predicted the right one). It couldn't accomodate the $\psi \to \gamma\chi$ rates (until the relativistic corrections were done).

The $b\bar{b}$ system is a good system to study: The rates and splittings are large enough to measure (although it isn't easy, and improvements are needed). And the theoretical calculations are more manageable than for $c\bar{c}$ (although more work is needed on higher-order QCD corrections, especially for Γ_{ggg}).

Don't wait for top, you're better off at the bottom (see Eichten's lectures at this school). There's plenty more to do: better measurements of the χ_b and especially χ_b', find the $^1P_1$ and η_b, ..., and hope for the things you aren't expecting!

Acknowledgements

I am indebted to my colleagues in the Crystal Ball collaboration for many useful discussions on this topic in the last years. In addition, I wish to thank S. Brodsky, W. Buchmüller, A. Martin, and M. Peskin for help on various theoretical points.

References

1. S. W. Herb *et al.*, Phys. Rev. Lett. **39** (1977), p. 252.
2. W. R. Innes *et al.*, Phys. Rev. Lett. **39** (1977), p. 1240; K. Ueno *et al.*, Phys. Rev. Lett. **42** (1979), p. 486.
3. Υ: Ch. Berger *et al.*(PLUTO), Phys. Lett. **76B** (1978), p. 243; C. W. Darden *et al.*(DASP II), Phys. Lett. **76B** (1978), p. 246; Υ': J. K. Bienlein *et al.*(DESY-Heid.) Phys. Lett. **78B** (1978), p. 360; C. W. Darden *et al.*(DASP II) Phys. Lett. **78B** (1978), p. 364.
4. D. Andrews *et al.*(CLEO), Phys. Rev. Lett. **44** (1980), p. 1108; T. Böhringer *et al.*(CUSB), Phys. Rev. Lett. **44** (1980), p. 1111.
5. D. Andrews *et al.*(CLEO), Phys. Rev. Lett. **45** (1980), p. 219; G. Finocchiaro *et al.*(CUSB), Phys. Rev. Lett. **45** (1980), p. 219.
6. D. Besson *et al.*(CLEO), preprint CLNS-84/629 CLEO-84-8 (1984).

7. D. M. J. Lovelock *et al.*(CUSB). Contributed Paper to the XXII International Conference on High Energy Physics, Leipzig, 1984 (unpublished), submitted to Phys. Rev. Lett.

8. S. I. Serednyakov *et al.*, JETP **44** (1976), p. 1063.

9. A. S. Artamonov *et al.*, Phys. Lett. **137B** (1984), p. 272.

10. W.W.MacKay *et al.*, Phys. Rev. D **29** (1984), p. 2483.

11. D. P. Barber *et al.*, Phys. Lett. **135B** (1984), p. 498.

12. J. Kutti, Proc. of Photon Lepton Symp., Cornell, 1983.

13. E. Eichten *et al.*, Phys. Rev. **D17** (1978), p. 3090; **D21** (1980), p. 203.

14. A. J. Buras *et al.*, Rev. Mod. Phys. **52** (1980), p. 199.

15. R. McClary and N. Byers, Phys. Rev. **D28** (1983), p. 1692; UCLA/TEP/83/11 (1983).

16. J. L. Richardson, Phys. Lett. **82B** (1979), p. 272.

17. W. Buchmüller, G. Grunberg and S.-H. H. Tye, Phys. Rev. Lett. **45** (1980), p. 103; erratum, p. 587; W. Buchmüller and S.-H. H. Tye, Phys. Rev. **D24** (1981), p. 132.

18. O. Abe, M. Haruyama, and A. Kanazawa, Phys. Rev. **D27** (1983), p. 675; K. Igi and K. Hikasa, Phys. Rev. **D28** (1983), p. 565; K. Hagiwara, S. Jacobs, M. G. Olsson, and K. J. Miller, Phys. Lett. **130B** (1983), p. 209.

19. M. Bander, D. Silverman, B. Klima, and U. Maor, Phys. Rev. **D29** (1984), p. 2038.

20. S. Gupta and S. Radford, Phys. Rev. **D24** (1981), p. 2309; **D25** (1982), p. 3430; S. Gupta, S. Radford, and W. W. Repko, Phys. Rev. **D26** (1982), p. 3305.

21. A. Martin, Phys. Lett. **93B** (1980), p. 338; **100B** (1981), p. 511; K. J. Miller and M. G. Olsson, Phys. Lett. **109B** (1982), p. 314.

22. R. Van Royen and V. Weisskopf, Nuovo Cimento **50** (1967), p. 617.

23. R. Barbieri, R. Gatto, R. Kögerler and Z. Kunszt, Phys. Lett. **57B** (1975), p. 455.

24. W. Celmaster, Phys. Rev. **D19** (1979), p. 1517.

25. Ch. Berger *et al.*(PLUTO), Z. Phys. C **1** (1979), p. 343.

26. P. Bock *et al.*(DESY-Heid.), Z. Phys. C **6** (1980), p. 125; by J. K. Bienlein *et al.*, Phys. Lett. **78B,** (1978), p. 360.

27. H. Albrecht *et al.*(DASP II), Phys. Lett. **116B** (1982), p. 383.

28. B. Niczyporuk *et al.*(LENA), Z. Phys. **C15** (1982), p. 299; Phys. Rev. Lett. **46** (1981), p. 92.

29. R. Giles *et al.*(CLEO), Phys. Rev. **D29** (1984), p. 1285.

30. B. Niczyporuk *et al.*(LENA), Phys. Lett. **99B** (1981), p. 169.

31. Ch. Berger *et al.*(PLUTO), Phys. Lett. **93B** (1980), p. 497.

32. D. Andrews *et al.*(CLEO), Phys. Rev. Lett. **50** (1983), p. 807.

33. J. J. Mueller *et al.*(CLEO), Phys. Rev. Lett. **46** (1981), p. 1181.

34. R. Giles *et al.*(CLEO), Phys. Rev. Lett. **50** (1983), p. 877.

35. J. E. Horstkotte *et al.*, (unpublished) CUSB-83-09 (1983).

36. H. Albrecht *et al.*(ARGUS), Phys. Lett. **134B** (1984).

37. S. Behrends *et al.*(CLEO), Phys. Rev. **D30** (1984), p. 1996.

38. H. Schroeder (ARGUS), Leipzig (1984).

39. P. B. Mackenzie and G. P. Lepage, Phys. Rev. Lett. **47** (1981), p. 1244; G. Grunberg, Phys. Lett. **95B,** (1980), p. 70.

40. S. J. Brodsky, G. P. Lepage, and P. B. Mackenzie, Phys Rev. **D28** (1983), p. 228.

41. R. D. Schamberger *et al.*(CUSB), Phys. Lett. **138B** (1984), p. 225.

42. P. Avery *et al.*(CLEO), (unpublished) CLNS 83/582 (1983).

43. E. Eichten and F. Feinberg, Phys. Rev. **D23**, p. 2724.

44. K. Han *et al.*(CUSB), Phys. Rev. Lett. **49** (1982), p. 1612; G. Eigen *et al.*, Phys. Rev. Lett. **49** (1982), p. 1616.

45. C. Klopfenstein *et al.*(CUSB), Phys. Rev. Lett. **51** (1983), p. 160; F. Pauss *et al.*, Phys. Lett. **130B** (1983), p. 439.

46. J. Irion (Crystal Ball), Invited Talk at the XIXth Rencontre de Moriond: New Particle Production, La Plagne, France, March 4-10, 1984, SLAC-PUB-3325; U. Volland, Leipzig, 1984.

47. P. Haas *et al.*(CLEO), Phys. Rev. Lett. **52** (1984), p. 799.